Pre-Clinical Research Report

Journal of INTERNATIONAL MEDICAL RESEARCH

Journal of International Medical Research
2019, Vol. 47(8) 3763–3777

DOI: 10.1177/0300060519842959
journals.sagepub.com/home/imr
SAGE

Effects of ricin on primary pulmonary alveolar macrophages

Zhendong Guo[1,*], Zhongyi Wang[1,*], Shanyu Meng[2], Zongzheng Zhao[1], Chunmao Zhang[1], Yingying Fu[1], Jiaming Li[1], Xin Nie[3], Cheng Zhang[1], Linna Liu[1], Bing Lu[1] and Jun Qian[1]

Abstract

Objective: We systematically investigated the cytotoxic effects of ricin in primary pulmonary alveolar macrophages (PAMs).

Methods: Primary PAMs were isolated from BALB/c mice. The cytotoxic effects of ricin were investigated *in vitro* by optical and transmission electron microscopy, detection of the inflammatory cytokine response, proteomic analysis, and subsequent biological functional analysis.

Results: Ricin induced shrinkage, apoptosis, vacuolization, and multi-organelle lesions in primary PAMs as demonstrated by optical and transmission electron microscopy. Ricin also induced a pronounced pro-inflammatory cytokine response in primary PAMs, including induction of tumor necrosis factor-α, interferon-γ, interleukin (IL)-1, IL-2, IL-6, IL-12, C-C motif chemokine ligand 2, and C-X-C motif chemokine ligand 2, while the anti-inflammatory cytokines IL-4 and IL-10 were less affected. Proteomic analysis and subsequent biological functional analysis identified eight proteins that were up/downregulated by ricin treatment and which might thus contribute to ricin toxicity. These proteins were involved in various functions, including redox, molecular chaperone, glycolysis, protein translation, and protein degradation functions.

Conclusion: The results of the present study further our understanding of the pathogenic mechanism of inhalational ricin poisoning.

[1]Academy of Military Medical Sciences, Beijing, China
[2]Agricultural and Biological Engineering Department, University of Florida, Gainesville, FL, USA
[3]No. 65316 Unit of PLA, Dalian, China

*These authors contributed equally to this work and are joint first authors.

Corresponding authors:
Linna Liu, Bing Lu, and Jun Qian, Academy of Military Medical Sciences, Beijing 100850, China.
Emails: liulinna777@126.com; 13693506666@163.com; qianj1970@126.com

Keywords
Ricin, pulmonary alveolar macrophage, cytotoxicity, pro-inflammatory cytokine response, proteomics, poisoning

Date received: 21 August 2018; accepted: 19 March 2019

Introduction

Ricin is a type II ribosome-inactivating protein that can be easily purified from the castor bean plant *Ricinus communis*. It is the most toxic phytotoxin and has been categorized as a Category B agent by the US Center for Disease Control and Prevention. Its high toxicity, low cost, and easy preparation make ricin a potential biological warfare agent,[1] and it has previously been used in multiple assassination attempts.[2] Ricin contains two polypeptide chains linked through a disulfide bridge. The A chain is the toxic moiety, which catalytically cleaves 28S rRNA and prevents the binding of elongation factor 2 (EF-2), resulting in termination of protein synthesis and cell death.[3] The B chain is the lectin moiety, which is responsible for transporting ricin into cells through binding primarily to the galactose residues of cell surface glycolipids or glycoproteins.[4] The A and B chains can also bind to mannose residues.[5,6]

Previous studies in rodents and non-human primates demonstrated that inhalation of aerosolized ricin caused severe lung lesions and acute respiratory distress syndrome.[7] Pulmonary alveolar macrophages (PAMs) play a central role in the mechanism of ricin toxicity.[8] Following pulmonary intoxication, inflammatory cells and neutrophils migrate to the lungs.[9] Ricin first encounters PAMs in the alveolar lumen and induces their apoptosis, resulting in a halving of the number of PAMs as early as 18 hours after intoxication.[10] Ricin then causes further necrosis of lung bronchiolar epithelial cells and type II alveolar cells, ultimately resulting in death due to respiratory failure.[11]

The PAMs present in the alveolus are immune cells that are responsible for fighting off invading pathogens, eliminating aged or damaged cells, and maintaining the organism's homeostasis. Macrophages are particularly sensitive to ricin because they express both galactose and mannose residues on their cell surface,[6,12] and are therefore frequently used to study the mechanism of ricin toxicity. Most previous studies have used tumor cell lines such as Raw 264.7 or J774A.1 cells;[13–15] however, the characteristics of tumor cell lines and normal cells differ,[16–18] and systematic research on ricin cytotoxicity using normal or primary cells is limited.

In the present study, we isolated primary PAMs from mice and evaluated the cytotoxic effects of ricin at the cellular, subcellular, gene, and protein levels. There are currently no licensed treatment options to prevent or cure ricin poisoning, and symptomatic therapy is one of the most widely used and effective strategies. The results of the present study clarify the response of primary PAMs to ricin and thus provide new insights to aid the future development of novel therapeutic drugs.

Materials and methods

Extraction of primary PAMs

Primary PAMs were isolated from healthy 6-week-old BALB/c female mice (Center of

Experimental Animals of Jilin University, Changchun, China). All animal studies were conducted in strict accordance with the Guide for the Care and Use of Laboratory Animals of the Academy of Military Medical Sciences. All animal experiments were approved by the Animal Care and Use Committee of the Academy of Military Medical Sciences (approval no. SCXK 20160008). The lungs were lavaged with 2 mL phosphate-buffered saline (PBS). The bronchoalveolar lavage fluid was washed three times by centrifugation at $140 \times g$ for 5 minutes and resuspended with RPMI 1640 medium supplemented with 10% fetal bovine serum, 100 U/mL penicillin, and 0.1 mg/mL streptomycin. The cell suspension was cultured at 37°C in a 5% CO_2 incubator with humidified air. Macrophages were purified by removing non-adherent cells following culture for 4 hours. All procedures were performed within a sterile environment.

Cell viability assay

The morphological characteristics of the cells were observed by staining with modified Wright–Giemsa stain (Sigma-Aldrich; Merck KGA, Darmstadt, Germany) according to the manufacturer's protocol.

The phagocytic activity of primary PAMs was determined by adding chicken erythrocytes to a final concentration of 10^4/mL and incubated for 12 hours. The degree of phagocytosis was then observed under an optical microscope (Nikon Corporation, Tokyo, Japan).

The half maximal inhibitory concentration (IC_{50}) of ricin (Sigma-Aldrich, Corp., St. Louis, MO, USA) was tested by MTS assay (Promega Corporation, Madison, WI, USA). In brief, the cells were grown in 96-well plates and treated with serially diluted ricin (0–10^5 ng/mL) for 12 hours, followed by the addition of 20 μL MTS to each well. After incubation for 2 hours at 37°C, the absorption was determined at 490 nm. All experiments were performed in triplicate.

Pathological analysis

Pathological lesions induced by ricin were observed at cellular and subcellular levels. For cellular-level observations, the cells were treated with 1 ng/mL ricin and observed under an optical microscope after 0, 6, and 12 hours at ×100, ×400, and ×600 magnifications. For observations at a subcellular level, the cells were treated with 1 ng/mL ricin for 12 hours and adherent cells were then collected by trypsinization. After three washes with PBS, the cells were centrifuged at $140 \times g$ for 5 minutes and resuspended with 2.5% glutaraldehyde fixative. The cells were then observed under a transmission electron microscope (JEOL, Ltd., Tokyo, Japan).

Analysis of cytokines and chemokines

Cytokine and chemokine gene expression levels in the cells were determined by real-time reverse transcription-quantitative polymerase chain reaction (RT-qPCR) assay. Total RNA was extracted from the cells using TRIzol reagent (Invitrogen; Thermo Fisher Scientific, Inc., Waltham, MA, USA). First-strand cDNA was synthesized from the total RNA using M-MLV (Takara Bio, Inc., Otsu, Japan) with oligo (dT)s for RT-PCR analysis. mRNA expression levels of the genes encoding tumor necrosis factor-α (TNF-α), interferon-γ (IFN-γ), interleukin (IL)-1α, IL-1b, IL-2, IL-4, IL-6, IL-10, IL-12b, C-C motif chemokine ligand 2 (CCL2), and C-X-C motif chemokine ligand 2 (CXCL2) were determined by RT-qPCR assays performed in triplicate using an Applied Biosystems 7500 Real-Time PCR system (Applied Biosystems; Thermo Fisher Scientific, Inc.) with SYBR Green Master mix (Takara Bio,

Table 1. Primer sequences used for quantitative real-time polymerase chain reaction assays.

Target	Primer sequence	
TNF-α	forward	5′-CATCTTCTCAAAATTCGAGTGACAA-3′
	reverse	5′-TGGGAGTAGACAAGGTACAACCC-3′
IFN-γ	forward	5′-ACCTGTTCTTTGAAGTTGACGGAC-3′
	reverse	5′-CTCCACAGCCACAATGAGTGATAC-3′
IL-1α	forward	5′-TGATGAAGCTCGTCAGGCAGAAGT-3′
	reverse	5′-TCTCCTCCCGACGAGTAGGCATA-3′
IL-1β	forward	5′-ACCTGTTCTTTGAAGTTGACGGAC-3′
	reverse	5′-CTCCACAGCCACAATGAGTGATAC-3′
IL-2	forward	5′-CCTGAGCAGGATGGAGAATTACA-3′
	reverse	5′-TCCAGAACATGCCGCAGAG-3′
IL-4	forward	5′-ACAGGAGAAGGGACGCCAT-3′
	reverse	5′-GAAGCCCTACAGACGAGCTCA-3′
IL-6	forward	5′-CAAAGCCAGAGTCCTTCAGAGAG-3′
	reverse	5′-GTCTTGGTCCTTAGCCACTCCTT-3′
IL-10	forward	5′-GGTTGCCAAGCCTTATCGGA-3′
	reverse	5′-ACCTGCTCCACTGCCTTGCT-3′
IL-12β	forward	5′-GGAAGCACGGCAGCAGAATA-3′
	reverse	5′-AACTTGAGGGAGAAGTAGGAATGG-3′
CCL2	forward	5′-GTTGGCTCAGCCAGATGCA-3′
	reverse	5′-AGCCTACTCATTGGGATCATCTTG-3′
CXCL2	forward	5′-CCCTGGTTCAGAAAATCATCC-3′
	reverse	5′-TCTCAGACAGCGAGGCACAT-3′
β-actin	forward	5′-CAACCGTGAAAAGATGACCCAG-3′
	reverse	5′-GACCAGAGGCATACAGGGACAG-3′

Inc.).[19] The mRNA levels were normalized against the β-actin housekeeping gene.[20,21] The primer sequences used for PCR are listed in Table 1. The expression of each mRNA relative to β-actin was determined using the $2^{-\Delta\Delta CT}$ method.[22,23]

Protein sample preparation, two-dimensional gel electrophoresis (2-DE) and matrix-assisted laser desorption/ionization-time of flight mass spectrometry (MALDI-TOF/MS) analysis

Ricin-treated (1 ng/mL) and control cells treated with PBS (12 hours post-exposure) were collected and suspended in lysis buffer (9.5 M urea, 4% CHAPS, 65 mM dithiothreitol, and 0.2% carrier ampholyte) containing a protease inhibitor cocktail (Roche Diagnostics GmbH, Mannheim, Germany). Following lysis for 30 minutes, the suspension was centrifuged at $30{,}428 \times g$ for 5 minutes at 4°C. The supernatant was collected and protein concentrations were determined using a Protein Assay kit (Bio-Rad Laboratories, Inc., Hercules, CA, USA). Protein aliquots equivalent to 100 mg were stored at −80°C prior to their use. Proteins were separated by 2-DE (Bio-Rad Laboratories, Inc.).[24] The 2-DE gels were scanned using a GS-710 imaging densitometer (Bio-Rad) and the digitized images were analyzed using PDQuest software (Bio-Rad). Protein spots were cut from the gels, destained, washed, and kept in 0.2 M NH_4HCO3 for 20 minutes, and then lyophilized. Each spot was digested overnight with 12.5 ng/mL trypsin in

0.1 M NH_4HCO_3, and the digested proteins were extracted three times with 50% Acetonitrile, 0.1% Trifluoroacetic acid solution. All mass spectra data were acquired using an AutoFlex MALDI-TOF/TOF mass spectrometer with LIFT technology (Bruker Daltonics, Bremen, Germany). MS/MS data were acquired with an N2 laser at a 25-Hz sampling rate. Peptide mass fingerprinting (PMF) and MS data were combined by FlexAnalysis and the combined data set was submitted to MASCOT for protein identification. MASCOT provides a probability-based Mowse score which is expressed as $-10 \times \log(P)$, where P is the probability. Protein scores >63 are considered statistically significant ($P < 0.05$). The above process was repeated three times. The criteria for selecting protein spots: (i) spots with >two-fold expression changes between control and experimental groups; (ii) reproducible spots detected in all three replicate experiments; and (iii) successful identification of spots using MALDI-TOF analysis. The functions of the proteins were determined by literature search.

Statistical analysis

Statistical analysis was performed using SAS software version 9.3 (SAS Institute, Inc., Cary, NC, USA). Cytokine/chemokine levels were compared using ANOVA, and comparisons between two groups were tested using the Student–Newman–Keuls method. $P < 0.05$ was considered to indicate a significant difference.

Results

Extraction and identification of primary PAMs

Primary PAMs were harvested by bronchoalveolar lavage from BALB/c mice. The lavage fluid mainly contained macrophages, lymphocytes, and erythrocytes (Figure 1a). The macrophages were further purified by collecting adherent cells after a short culture period. Wright–Giemsa staining revealed a high degree of purity (Figure 1b).

The phagocytic activity of the purified macrophages was assessed by adding chicken erythrocytes to the culture dish. The macrophages engulfed the erythrocytes within 12 hours (Figure 1c). The primary PAMs were also sensitive to ricin, with an IC_{50} of 1 ng/mL (Figure 1d). These results confirmed that the purified primary PAMs demonstrated high phagocytic activity and purity.

Pathological observation of primary PAMs treated with ricin

Cellular level. Pathological lesions in PAMs were detected at the cellular level by optical microscopy. Control PAMs were morphologically intact with high vigor, good light transmittance, pleomorphism, and pseudopodia (Figure 2a-c). In contrast, cells treated with ricin began to shrink after 6 hours, and cellular adherence and light transmittance were reduced compared with the control cells (Figure 2d). At 6 hours post-inoculation with ricin, some cells showed signs of apoptosis, with fragmented cells (Figure 2e) and apoptotic bodies (Figure 2f). The lesions had progressed by 12 hours post-inoculation with ricin, and most cells exhibited shrinkage, with markedly reduced light transmittance and cellular adhesion (Figure 2g). The number of apoptotic cells and fused macrophages had also markedly increased at 12 hours post-inoculation (Figure 2h) and foam-like cells with vacuoles were also observed (Figure 2i).

Subcellular level. Pathological lesions in PAMS were detected at the subcellular level by transmission electron microscopy. The cytoplasm in control cells was uniform,

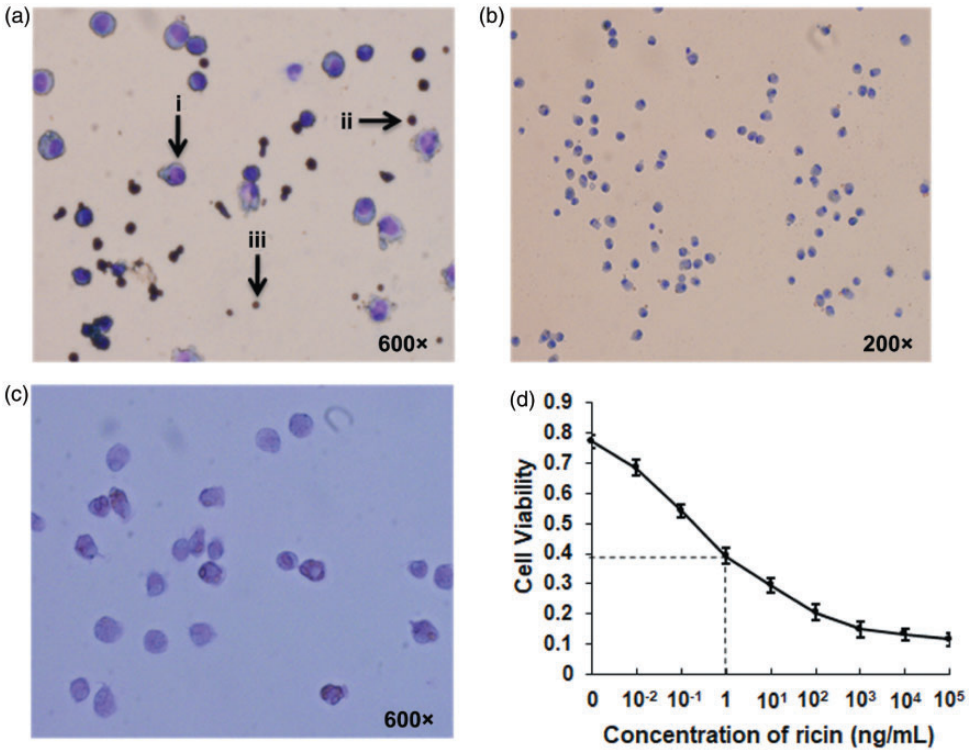

Figure 1. Extraction and identification of primary pulmonary alveolar macrophages (PAMS). (a) Wright-Giemsa stain revealed that the lung lavage fluid primarily contained (i) macrophages, (ii) lymphocytes, and (iii) erythrocytes. (b) Selection of adherent cells produced primary PAMs with high purity. (c) Primary PAMs engulfed chicken erythrocytes, indicating good phagocytic activity. (d) The half maximal inhibitory concentration (IC_{50}) of ricin in primary PAMs was 1 ng/mL according to MTS assay.

the filopodia were arranged neatly (Figure 3a), and the organelle structures were normal (Figure 3b). By 12 hours post-inoculation with ricin, the primary PAMs showed vacuolization with increased filopodia and various stages of lysosome development were apparent (Figure 3c and d). Myeloid bodies, cotton-like deposition, and cytocannibalism were also observed (Figure 3e). The cell nucleus became smaller and showed degeneration, heterochromatin deposition, and nucleolar margination (Figure 3c and f). Electron-dense deposits appeared in the cytoplasm (Figure 3g). The numbers of mitochondria were depleted and vacuoles and electron-dense deposits appeared. The mitochondrial membrane was partially broken and indistinct (Figure 3h). The endoplasmic reticulum (ER) and Golgi apparatus were dilated (Figure 3i and j) and the ribosomes of the rough ER had partly shed (Figure 3h).

Ricin induced a pronounced pro-inflammatory cytokine response in primary PAMs. Inoculation of primary PAMs with ricin caused hyperinduction of the host pro-inflammatory response (Figure 4). mRNA levels of TNF-α, IFN-γ, IL-1α, IL-1β, IL-2, IL-6, IL-12β, and CXCL2 gradually increased and peaked at 9 hours post-inoculation (30.02, 94.33, 667.67, 135.02,

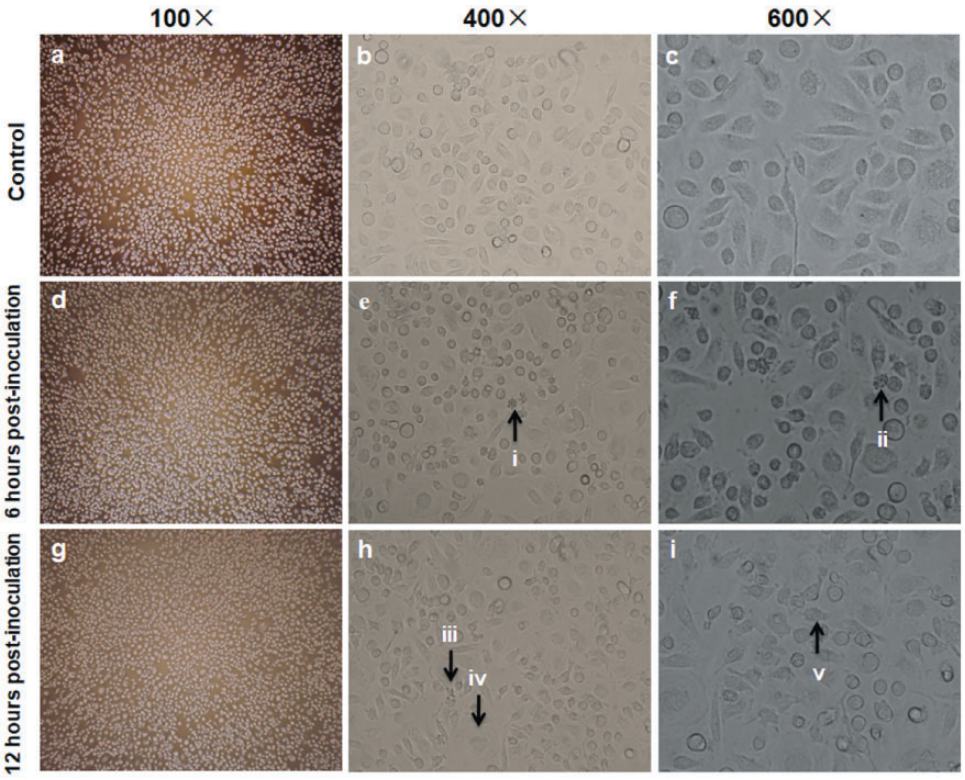

Figure 2. Morphology and viability of primary pulmonary alveolar macrophages (PAMs) following treatment with ricin. PAMs were treated with 1 ng/mL ricin and observed under an optical microscope at 0, 6, and 12 hours at ×100, ×400, and ×600 magnification. (a–c) Control PAMs were morphologically intact with high vigor, good light transmittance, pleomorphism, and pseudopodia. (d) At 6 hours post-inoculation with ricin the cells began to shrink and there showed reduced cellular adherence with lower light transmittance. (e) Some cells showed signs of apoptosis, with fragmented cells and (f) apoptotic bodies. (g) The lesions had progressed at 12 hours post-inoculation with ricin, and most cells exhibited shrinkage, reduced light transmittance and adhesion. (h) Apoptotic cells and fused macrophages increased and (i) foam-like cells with vacuoles were observed. i, fragmented cells; ii, apoptotic body; iii, apoptotic cell; iv, fused macrophages; v, foam-like cell.

30.08, 185.31, 13.84, and 386.41-fold increases, respectively; all $P < 0.05$ compared with baseline). CCL2 was also upregulated and peaked at 6 hours post-inoculation (8.76-fold increase; $P < 0.05$). Levels of the anti-inflammatory cytokines IL-4 and IL-10 were less affected by ricin (less than two-fold changes).

Proteome analysis of primary PAMs treated with ricin. The differential expression of proteins in primary PAMs incubated with ricin was further investigated using proteomics. A total of 10 proteins were clearly differentially expressed between the ricin and control groups based on the results of 2-DE (Figure 5a and b) and PDQuest software analysis (Figure 5c) (Table 2). A more detailed view is shown in Figure 6. The proteins were enzymatically hydrolyzed and subjected to MALDI-TOF/MS, which successfully identified the proteins (Table 3). The differentially expressed proteins were involved in various functions, including

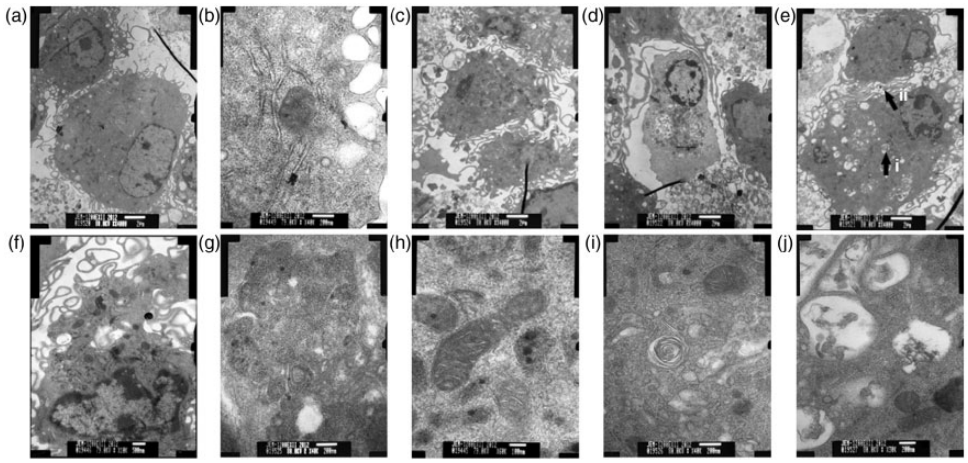

Figure 3. Pathological lesions in primary pulmonary alveolar macrophages (PAMs) induced by ricin. PAMs were treated with 1 ng/mL ricin for 12 hours and adherent cells were collected, washed, resuspended with 2.5% glutaraldehyde, and observed under a transmission electron microscope. a and b, control group; c–j, ricin-treated group; i, myeloid body; ii, cytocannibalism.

redox, blood homeostasis, molecular chaperone, glycolysis, protein translation, and protein degradation functions.

Discussion

The lungs are the body's respiratory organ and are responsible for gas exchange with the external environment, making them susceptible to invasion by aerosolized pathogens. PAMs are the primary phagocytes of the immune systems and serve an important role in maintaining lung homeostasis, eliminating exogenous pathogens, and regulating immune responses by secreting multiple cytokines. Primary cells are isolated directly from a living organism and their biological characteristics are therefore considered to be similar to cells within the body. Physiological and immune response tests using primary cells are therefore more likely to yield representative results than similar tests using tumor cell lines, and may be more helpful in terms of understanding the body's response mechanisms. Inhalation of ricin has previously been shown to induce severe pulmonary lesions, and PAMs have demonstrated an important role in this process.[8] In the present study, we therefore isolated primary PAMs from mice by bronchoalveolar lavage and evaluated the cytotoxic effects of ricin in these primary PAMs.

Ricin induced a pronounced pro-inflammatory cytokine response in the primary PAMs, which was consistent with the results of previous studies. Meghan et al.[25] observed that macrophages served a central role in the pulmonary inflammatory process triggered by ricin, while Licastro et al.[26] revealed that ricin induced the release of TNF-α and IL-1β by human peripheral-blood mononuclear cells. TNF-α was also upregulated in J744A.1 macrophages[14] and RAW 264.7 cells.[15] Ricin inhalation has been shown to transcriptionally activate pulmonary gene expression of IL-6 in BALB/c mice.[27] However, previous studies only examined a few pro-inflammatory cytokines, and information on the effects of ricin on the induction of pro-inflammatory cytokines in primary PAMs

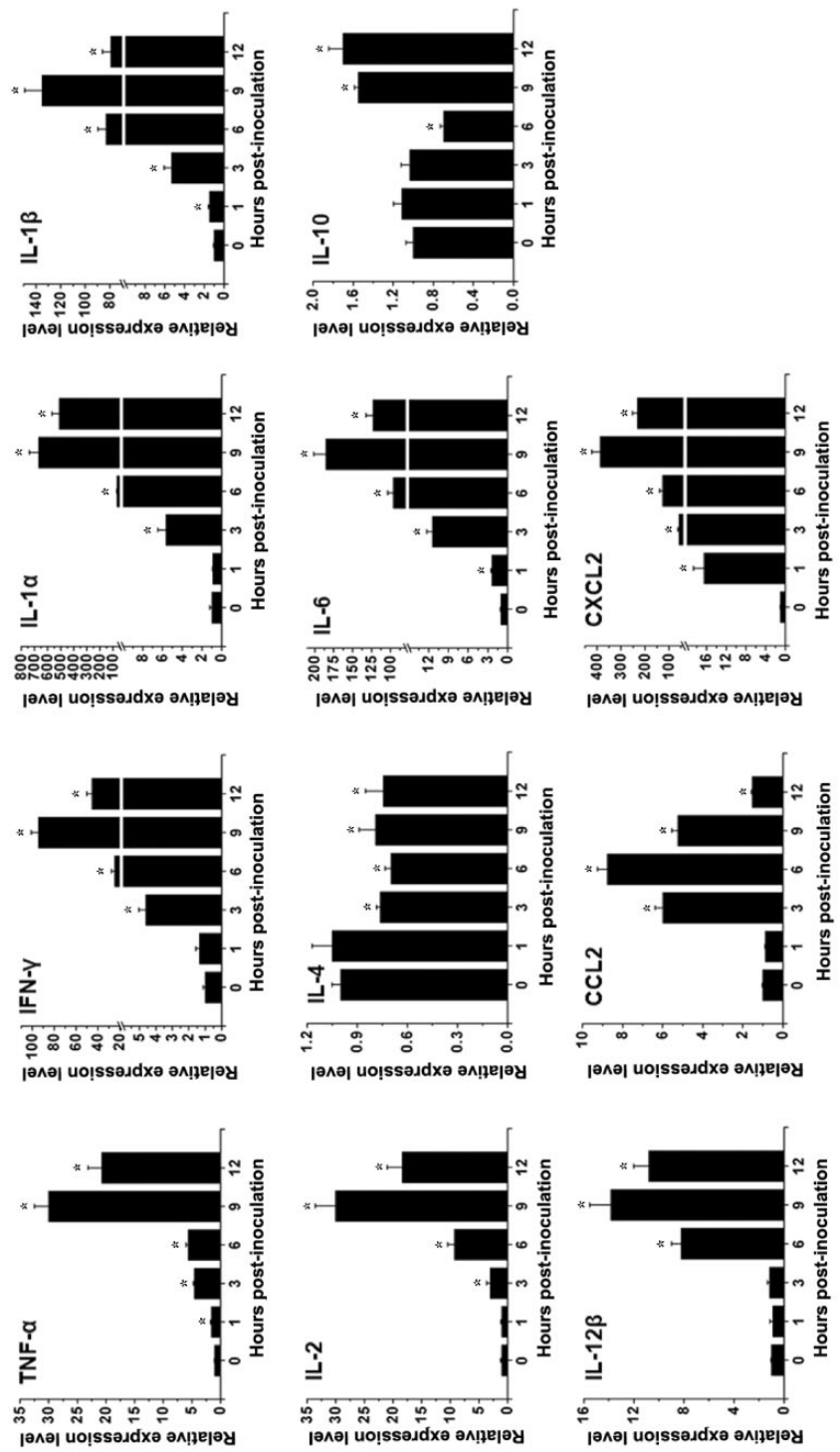

Figure 4. Cytokine and chemokine mRNA levels in primary pulmonary alveolar macrophages inoculated with ricin. Experiments were performed in triplicate. Data presented as mean ± standard error of the mean. *$P < 0.05$ vs. 0 hour group.

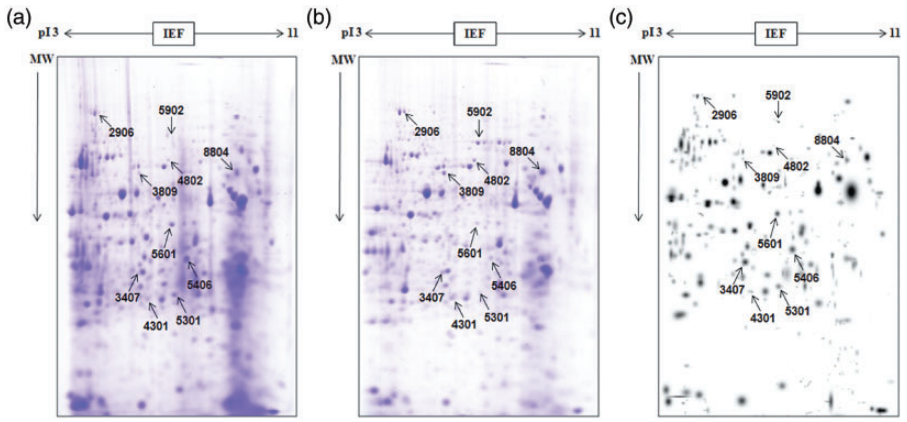

Figure 5. Proteomic analysis of primary pulmonary alveolar macrophages treated with ricin. Proteins in (a) the control group and (b) the ricin-treated group were separated by two-dimensional electrophoresis, visualized using Coomassie Blue staining, (c) and analyzed using PDQuest software. The spots representing significantly different protein expression levels (arrows) were selected for further mass spectrometric analysis. More detailed views are shown in Figure 6.

Table 2. Numerical values of protein spots with differential expressions were analyzed using PDQuest software.

SSP	Group C	Group E
2906	914.1	5644.8
3407	440.1	10562.2
3809	2047.3	11663.0
4301	3227.9	6725.7
4802	656.3	7544.5
5301	12760.0	0
5406	27866.6	6996.4
5601	17847.5	5613.7
5902	2982.1	10791.2
8804	6148.7	14885.8

Standard spot (SSP) numbers were assigned to each protein spot by PDQuest software. Each SSP number uniquely identifies one protein. Group C: control group, Group E: ricin-treated group.

is lacking. In the current study, we analyzed the effects of ricin on numerous inflammation-related cytokines, including TNF-α, IFN-γ, IL-1α, IL-1β, IL-2, IL-4, IL-6, IL-10, IL-12β, CCL2, and CXCL2, thus providing important additional information on the mechanisms of ricin damage though aerosol contamination. Furthermore, the use of primary PAMs means that the results might better represent the immune responses in the lung following inhalational ricin exposure.

Ten proteins were shown to be significantly differentially expressed in ricin-treated compared with control primary PAMs. Subsequent biological functional analysis revealed that eight of them might potentially contribute to ricin toxicity, though further studies are needed to clarify their roles.

Protein disulfide-isomerase (PDI) is a multi-functional thioredoxin located in the plasma membrane, secretory vesicles, the Golgi apparatus, and most abundantly in the ER.[28] PDI was previously revealed to be involved in the reduction of ricin to its composite A and B chains in the ER,[29,30] and may also regulate the retro-translocation of cholera toxin.[31] The increased expression of PDI observed in ricin-treated primary PAMs warrants further investigation.

T-complex protein-1 (TCP-1) was up-regulated in ricin-treated primary PAMs.

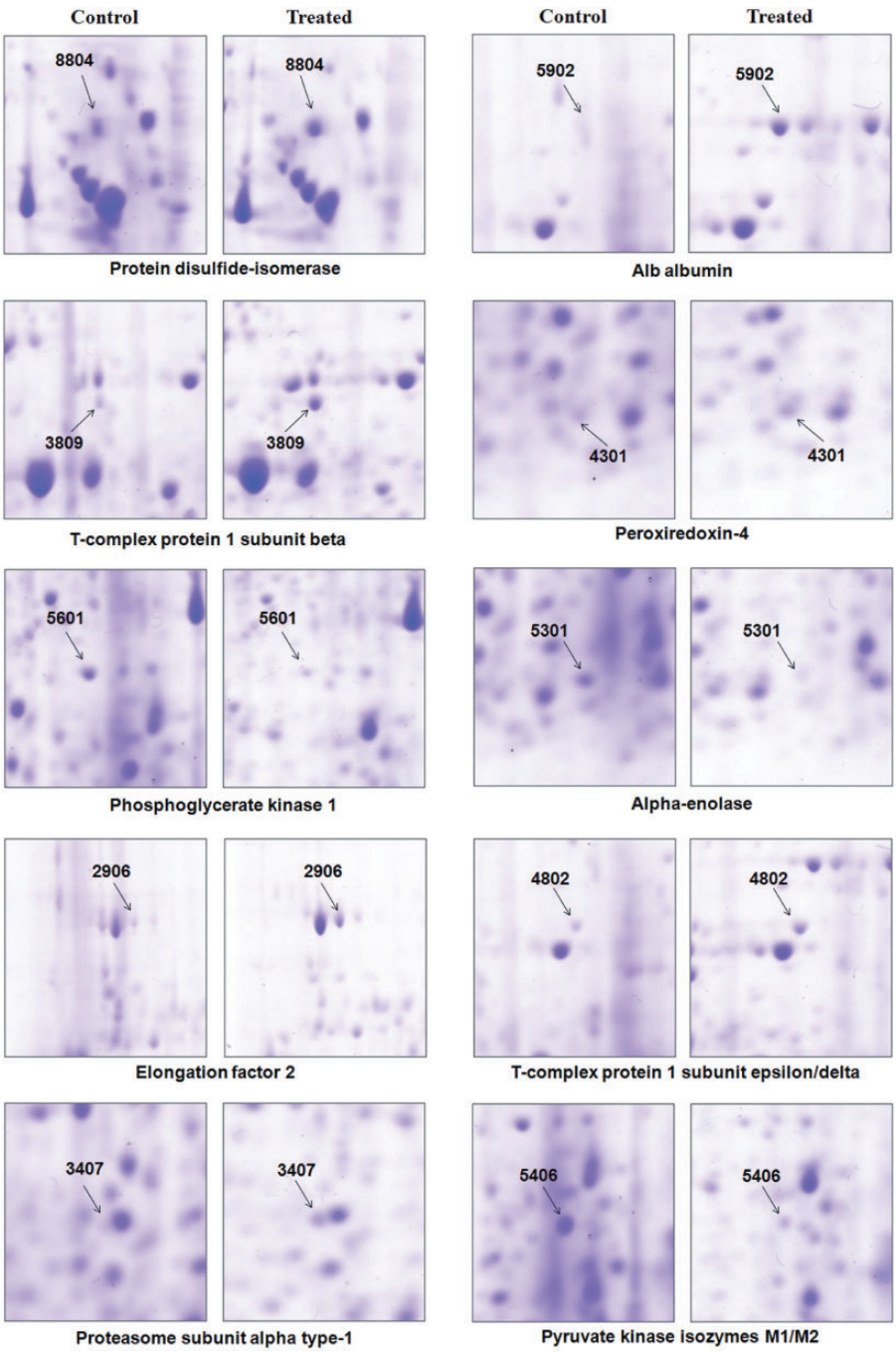

Figure 6. Segments of two-dimensional electrophoresis gel maps derived from control and ricin-treated primary pulmonary alveolar macrophages. Arrows indicate differentially expressed proteins.

Table 3. MALDI-TOF/MS identification of differentially expressed proteins.

SSP	NCBI Accession number	Name	MW (KDa)	Isoelectric point	Up/down-regulated	Function
8804	NP_035162	Protein disulfide-isomerase	57.4	4.77	Up	Redox
5902	CAD29888	Alb Serum albumin	70.7	5.75	Up	Blood homeostasis
3809	NP_031662	T-complex protein 1 subunit beta	57.8	5.97	Up	Molecular chaperone
4802	NP_031663/ NP_033967	T-complex protein 1 subunit epsilon/delta	60.0/58.5	5.72/8.24	Up	Molecular chaperone
4301	AAH19578	Peroxiredoxin 4	31.3	6.67	Up	Redox
5601	NP_032854	Phosphoglycerate kinase 1	44.9	8.02	Down	Glycolysis
5301	NP_075608	Alpha-enolase	47.5	6.37	Down	Glycolysis
2906	NP_031933	Elongation factor 2	96.2	6.41	Up	Protein translation
3407	NP_036095	Proteasome subunit alpha type-1	29.8	6.00	Up	Protein degradation
5406	NP_035229	Pyruvate kinase isozymes M1/M2	58.4	7.18	Down	Glycolysis

SSP: standard spot number.

TCP-1 is a molecular chaperone and a member of the chaperonin-containing TCP1 complex, also known as the TCP1 ring complex, which consists of two identical stacked rings, each containing eight different proteins. It assists in the folding of proteins in an ATP-dependent manner. This chaperonin complex has previously been shown to be required for the efficient delivery of anthrax toxin into the cytosol of host cells,[32] and was upregulated in mouse macrophages treated with anthrax toxin.[33] A systematic mammalian genetic interaction map revealed that knockdown of TCP-1 significantly increased the sensitivity of mammalian cells to ricin,[34] suggesting that an increase in TCP-1 expression levels may be one mechanism by which primary PAMs are able to withstand ricin.

Peroxiredoxins (PRDXs) comprise an extended family of small antioxidant proteins with a conserved thioredoxin-dependent catalytic function, which help to protect cells from reactive oxygen species.[35,36] PRDXs are classified as PRDX 1–6, and protect cellular components through their antioxidant functions. A previous study reported that ricin induced oxidative stress in the livers of mice and increased lipid peroxidation and superoxide production.[37,38] In the present study, PRDX 4 was upregulated in ricin-treated primary PAMs, suggesting that it might be involved in a protective mechanism to counter ricin-induced oxidative stress.

Expression levels of phosphoglycerate kinase 1 (PGK-1), α-enolase (ENO-1), and pyruvate kinase isozymes M1/M2 (PK-M1/M2) were decreased in the presence of ricin. These are all glycolysis-associated proteins that serve critical roles within the glycolytic signaling pathway. PGK-1 catalyzes the transfer of high-energy phosphate from the 1-position of 1,3 diphosphoglycerate (1,3-DPG) to ATP, converting 1,3-DPG into 3-phosphoglyceric acid.[39] ENO-1 catalyzes the dehydration of 2-phosphoglycerate to phosphoenolpyruvate in the last steps of the catabolic glycolytic signaling pathway,[40] while PK-M1/2 catalyzes the transfer of a phosphoryl group from phosphoenolpyruvate to ADP, generating pyruvate and ATP. These results indicate that ricin may target cellular energy metabolism, reducing cell vitality and contributing to cell death.

EF-2 serves an important role in eukaryotic polypeptide chain elongation by catalyzing the translocation of peptidyl-tRNA on the ribosome.[41] The ricin A chain

inactivates 28S ribosomal RNA and prevents the binding of EF-2, resulting in termination of protein synthesis and cell death. EF2 was previously shown to have a protective effect against the inactivation of ribosomes by the ricin A chain.[42] The upregulation of EF-2 in ricin-treated primary PAMs may thus help to counteract the ricin-induced termination of protein synthesis.

The proteasome is a multi-functional protease complex that cleaves most cytosolic proteins, regulates protein turnover, and maintains cellular homoeostasis.[43] Previous studies have demonstrated that mammalian cells can be sensitized after knockdown of the proteasome or inhibition of its proteolytic activities.[34,44] The increased proteasome expression observed in the present study may thus act as a protective mechanism to prevent the aggregation of unfolded ricin A chain.[43,45]

This study had some limitations. Notably, the purity of the primary PAMs was only demonstrated using Wright–Giemsa staining, and further studies using additional cell-detection methods are required to confirm the results. More studies are also needed to clarify the mechanisms and roles of these differentially expressed proteins.

The results of the present study conducted in primary PAMs clarify the pathological lesions caused by ricin and identify important cytokine and protein changes potentially associated with ricin toxicity. These findings contribute to an improved understanding of the pathogenesis of ricin toxicity and may aid the development of novel agents to prevent or treat ricin intoxication.[46]

Availability of data and materials

All data generated or analyzed during this study are included in this published article.

Declaration of conflicting interest

The authors declare that there is no conflict of interest.

Funding

This work was supported by the National Natural Science Foundation of China (grant no. 31101858). The funders had no role in study design, data collection and analysis, decision to publish, or preparation of the manuscript.

ORCID iD

Zhongyi Wang https://orcid.org/0000-0002-8982-2806

References

1. Crompton R and Gall D. Georgi Markov–death in a pellet. *Med Leg J* 1980; 48: 51–62.
2. Kevles DJ. The poor man's atomic bomb. *New York Rev Books* 2007; 54: 60–63.
3. Endo Y, Mitsui K, Motizuki M, et al. The mechanism of action of ricin and related toxic lectins on eukaryotic ribosomes. The site and the characteristics of the modification in 28 S ribosomal RNA caused by the toxins. *J Biol Chem* 1987; 262: 5908–5912.
4. Olsnes S and Kozlov JV. Ricin. *Toxicon* 2001; 39: 1723–1728.
5. Riccobono F and Fiani ML. Mannose receptor dependent uptake of ricin A1 and A2 chains by macrophages. *Carbohydr Res* 1996; 282: 285–292.
6. Simmons BM, Stahl PD and Russell JH. Mannose receptor-mediated uptake of ricin toxin and ricin A chain by macrophages. Multiple intracellular pathways for a chain translocation. *J Biol Chem* 1986; 261: 7912–7920.
7. Greenfield RA, Brown BR, Hutchins JB, et al. Microbiological, biological, and chemical weapons of warfare and terrorism. *Am J Med Sci* 2002; 323: 326–340.
8. Korcheva V, Wong J, Lindauer M, et al. Role of apoptotic signaling pathways in regulation of inflammatory responses to ricin in primary murine macrophages. *Mol Immunol* 2007; 44: 2761–2771.

9. Brown RF and White DE. Ultrastructure of rat lung following inhalation of ricin aerosol. *Int J Exp Pathol* 1997; 78: 267–276.
10. Sapoznikov A, Falach R, Mazor O, et al. Diverse profiles of ricin-cell interactions in the lung following intranasal exposure to ricin. *Toxins (Basel)* 2015; 7: 4817–4831.
11. Roy CJ, Hale M, Hartings JM, et al. Impact of inhalation exposure modality and particle size on the respiratory deposition of ricin in BALB/c mice. *Inhal Toxicol* 2003; 15: 619–638.
12. Battelli MG, Musiani S, Monti B, et al. Ricin toxicity to microglial and monocytic cells. *Neurochem Int* 2001; 39: 83–93.
13. Xu N, Yuan H, Liu W, et al. Activation of RAW264.7 mouse macrophage cells in vitro through treatment with recombinant ricin toxin-binding subunit B: involvement of protein tyrosine, NF-kappaB and JAK-STAT kinase signaling pathways. *Int J Mol Med* 2013; 32: 729–735.
14. Hassoun E and Wang X. Ricin-induced toxicity in the macrophage J744A.1 cells: the role of TNF-alpha and the modulation effects of TNF-alpha polyclonal antibody. *J Biochem Mol Toxicol* 2000; 14: 95–101.
15. Higuchi S, Tamura T and Oda T. Cross-talk between the pathways leading to the induction of apoptosis and the secretion of tumor necrosis factor-alpha in ricin-treated RAW 264.7 cells. *J Biochem* 2003; 134: 927–933.
16. Kraan J, van den Broek P, Verhoef C, et al. Endothelial CD276 (B7-H3) expression is increased in human malignancies and distinguishes between normal and tumour-derived circulating endothelial cells. *Br J Cancer* 2014; 111: 149–156.
17. Kobayashi K, Ohno S, Uchida S, et al. Cytotoxicity and type of cell death induced by local anesthetics in human oral normal and tumor cells. *Anticancer Res* 2012; 32: 2925–2933.
18. Hong X, Wang Q, Yang Y, et al. Gap junctions propagate opposite effects in normal and tumor testicular cells in response to cisplatin. *Cancer Lett* 2012; 317: 165–171.
19. Wang Z, Li J, Qian L, et al. Composition and distribution analysis of bioaerosols under different environmental conditions. *J Vis Exp* 2019; 143: e58795.
20. Fu Y, Wang Z, Lu B, et al. Immune response and differentially expressed proteins in the lung tissue of BALB/c mice challenged by aerosolized Brucella melitensis 5. *J Int Med Res* 2018; 46: 4740–4752.
21. Wang Z, Li J, Fu Y, et al. A rapid screen for host-encoded miRNAs with inhibitory effects against ebola virus using a transcription- and replication-competent virus-like particle system. *Int J Mol Med* 2018; 19: pii: E1488.
22. Guo Z, Wang Z, Qian LA, et al. Biological and chemical compositions of atmospheric particulate matter during hazardous haze days in Beijing. *Environ Sci Pollut Res Int* 2018; 25: 34540–34549.
23. Wang ZY, Guo ZD, Li JM, et al. Genome-wide search for competing endogenous RNAs responsible for the effects induced by ebola virus replication and transcription using a trVLP system. *Front Cell Infect Microbiol* 2017; 7: 479.
24. Mizushima N and Komatsu M. Autophagy: renovation of cells and tissues. *Cell* 2011; 147: 728–741.
25. Lindauer ML, Wong J, Iwakura Y, et al. Pulmonary inflammation triggered by ricin toxin requires macrophages and IL-1 signaling. *J Immunol* 2009; 183: 1419–1426.
26. DaSilva L, Cote D, Roy C, et al. Pulmonary gene expression profiling of inhaled ricin. *Toxicon* 2003; 41: 813–822.
27. Akagi S, Yamamoto A, Yoshimori T, et al. Localization of protein disulfide isomerase on plasma membranes of rat exocrine pancreatic cells. *J Histochem Cytochem* 1988; 36: 1069–1074.
28. Spooner RA, Watson PD, Marsden CJ, et al. Protein disulphide-isomerase reduces ricin to its A and B chains in the endoplasmic reticulum. *Biochem J* 2004; 383: 285–293.
29. Bellisola G, Fracasso G, Ippoliti R, et al. Reductive activation of ricin and ricin A-chain immunotoxins by protein disulfide isomerase and thioredoxin reductase. *Biochem Pharmacol* 2004; 67: 1721–1731.
30. Moore P, Bernardi KM and Tsai B. The Ero1alpha-PDI redox cycle regulates retrotranslocation of cholera toxin. *Mol Biol Cell* 2010; 21: 1305–1313.

31. Slater LH, Hett EC, Clatworthy AE, et al. CCT chaperonin complex is required for efficient delivery of anthrax toxin into the cytosol of host cells. *Proc Natl Acad Sci U S A* 2013; 110: 9932–9937.
32. Chandra H, Gupta PK, Sharma K, et al. Proteome analysis of mouse macrophages treated with anthrax lethal toxin. *Biochim Biophys Acta* 2005; 1747: 151–159.
33. Bassik MC, Kampmann M, Lebbink RJ, et al. A systematic mammalian genetic interaction map reveals pathways underlying ricin susceptibility. *Cell* 2013; 152: 909–922.
34. Wood ZA, Schroder E, Robin Harris J, et al. Structure, mechanism and regulation of peroxiredoxins. *Trends Biochem Sci* 2003; 28: 32–40.
35. Hofmann B, Hecht HJ and Flohe L. Peroxiredoxins. *Biol Chem* 2002; 383: 347–364.
36. Muldoon DF, Hassoun EA and Stohs SJ. Ricin-induced hepatic lipid peroxidation, glutathione depletion, and DNA single-strand breaks in mice. *Toxicon* 1992; 30: 977–984.
37. Muldoon DF, Hassoun EA and Stohs SJ. Role of iron in ricin-induced lipid peroxidation and superoxide production. *Res Commun Mol Pathol Pharmacol* 1996; 92: 107–118.
38. Beutler E. PGK deficiency. *Br J Haematol* 2007; 136: 3–11.
39. Pancholi V. Multifunctional alpha-enolase: its role in diseases. *Cell Mol Life Sci* 2001; 58: 902–920.
40. Merrick WC and Nyborg J. The Protein Biosynthesis, Elongation Cycle. In: Sonenberg N, Hershey JWB and Mathews MB (eds) *Translational Control of Gene Expression*. Cold Spring Harbor Laboratory Press, 2000, pp.89–125.
41. Fernandez-Puentes C, Benson S, Olsnes S, et al. Protective effect of elongation factor 2 on the inactivation of ribosomes by the toxic lectins abrin and ricin. *Eur J Biochem* 1976; 64: 437–443.
42. Pietroni P, Vasisht N, Cook JP, et al. The proteasome cap RPT5/Rpt5p subunit prevents aggregation of unfolded ricin A chain. *Biochem J* 2013; 453: 435–445.
43. Deeks ED, Cook JP, Day PJ, et al. The low lysine content of ricin A chain reduces the risk of proteolytic degradation after translocation from the endoplasmic reticulum to the cytosol. *Biochemistry* 2002; 41: 3405–3413.
44. Wesche J, Rapak A and Olsnes S. Dependence of ricin toxicity on translocation of the toxin A-chain from the endoplasmic reticulum to the cytosol. *J Biol Chem* 1999; 274: 34443–34449.
45. Meneguelli de Souza LC, Carvalho LP, Araujo JS, et al. Cell toxicity by ricin and elucidation of mechanism of Ricin inactivation. *Int J Mol Med* 2018; 113: 821–828.
46. Roy CJ, Ehrbar DJ, Bohorova N, et al. Rescue of rhesus macaques from the lethality of aerosolized ricin toxin. *JCI Insight* 2019; 4: pii: 124771.